ARMA Modeling for Estimation of Permeability from Perfusion MRI

Mohammad Mehdi Khalighi[1,2], Hamid Soltanian-Zadeh[1,2], James R. Ewing[3]
[1]Electrical and Computer Engineering Department, University of Tehran, Tehran, Iran
[2]Radiology Image Analysis Lab, Henry Ford Health System, Detroit, MI 48202
[3]Neurology Department, Henry Ford Health System, Detroit, MI 48202

ABSTRACT

We develop noninvasive MRI techniques that quantify the permeability of the Blood-Brain Barrier (BBB). Using such gadolinium compounds as Gd-DTPA and gadomer-17, changes in R1 (R1 = 1/T1) can be measured and used as estimates of tissue concentration *versus* time, thus permitting estimates of BBB permeability parameters. Estimating BBB permeability parameters requires deconvolution in a linear system, a task that has been accomplished heretofore by nonlinear least-squares procedures[1-3], although these techniques tend to instability in the presence of noise. We introduce a method using Z-transform and Autoregressive Moving Average (ARMA) modeling to perform this deconvolution. This method has the advantage that it linearizes the optimization procedure by which parametric estimates are formed, and it stabilizes the deconvolution in the presence of noise.

Keywords: auto regressive moving average, ARMA, Z-transform, permeability, perfusion, magnetic resonance imaging, MRI

1. INTRODUCTION

Most proposals to quantitate BBB permeability have used a compound of gadolinium as the indicator, and some T1-related magnetic resonance imaging (MRI) parameter to judge tissue concentration of the gadolinium. Early proposals for the quantitation of BBB permeability have emerged from Tofts and Kermode [2] Larsson et. al. [4], and Brix et. al. [5]. Tofts, in reviews [1,6], has noted the differences between these approaches, and resolved differences in notation. Common to these approaches is the assumption that contrast changes due to magnetic resonance contrast agent (MRCA) in the vascular volume are negligible. This assumption is challenged by Henderson et al [3]; these authors present the full model and demonstrate maps of BBB permeability parameters using fast T1-weighted imaging procedures. We have adopted their model, but used slower imaging techniques to estimate changes in R1, which have been shown to be proportional to tissue concentration of Gd [2]. In order to optimize our parametric estimation, we have sought stable approaches to deconvolution in the presence of noise.

2. METHODS

2.1 Theory

The goal is to estimate the quantity of indicator inside and outside the capillary bed. This is approached via a single capillary model [7,8]. After the distribution of indicator in the capillary is considered, the concentration of indicator in the tissue can be inferred. We will use the so-called adiabetic approximation [9] and consider that the concentration in the tissue changes very slowly when compared to the concentration in the capillary. So the concentration of agent in the tissue can be written as [3]:

$$C_{tis}(t) = rC_a(t) \otimes FE' e^{-\frac{FE'}{V_{ees}}t} + r\alpha \quad C_a(t) \qquad (1)$$

where C_a is the plasma concentration of indicator at the entrance to the capillary, F is the capillary flow (ml/min) V_{ees} is the fraction tissue volume (ml/gr) occupied by the extracellular indicator, E' is the extraction fraction in where there is no extravascular concentration of indicator, i.e., the portion of indicator that leaks out of the capillary in a single pass, r is the constant of proportion relating arterial concentration of indicator to capillary concentration and α is the vascular fraction in tissue (ml/g). In a real experiment we always have noise and so we can re-write equation (1) as:

$$C_{tis}(t) = rC_a(t) \otimes FE' e^{-\frac{FE'}{V_{ees}}t} + r\alpha \quad C_a(t) + e(t) \qquad (2)$$

where $e(t)$ is random white noise. This equation is in continuous time domain and if we sample $C_{tis}(t)$ and $C_a(t)$ each T seconds, then in discrete time domain we have:

$$C_{tis}(n) = rC_a(n) \otimes FE' e^{-\frac{FE'T}{V_{ees}}n} + r\alpha \quad C_a(n) + e(n) \qquad (3)$$
$$n = 0,1,\ldots, N-1$$

Taking the Z-transform of equation (3), we get:

$$C_{tis}(Z) = rC_a(Z) \cdot Z\left\{FE^{'} \cdot e^{-\frac{FE^{'}T}{V_{ees}}n}\right\} + r\alpha \quad C_a(Z) + E(Z) \qquad (4)$$

where $C_{tis}(Z)$, $C_a(Z)$, and $E(Z)$ are the Z-transforms of $C_{tis}(t)$, $C_a(t)$, and $e(t)$, respectively. The Z-transform of the kernel is:

$$Z\left\{FE^{'} \cdot e^{-\frac{FE^{'}T}{V_{ees}}n}\right\} = FE^{'}\sum_{n=0}^{\infty} e^{-\frac{FE^{'}T}{V_{ees}}n} Z^{-n} = \frac{FE^{'}}{1 - e^{-\frac{FE^{'}T}{V_{ees}}} Z^{-1}} \qquad (5)$$

If the system's pole located at $Z = e^{-\frac{FE^{'}T}{V_{ees}}}$ is inside the unit circle $(e^{-\frac{FE^{'}T}{V_{ees}}} < 1)$ then the region of convergence (ROC) includes the unit circle $(|Z| = 1)$. Substituting (5) in (4) results in:

$$C_{tis}(Z) = C_a(Z) \cdot \frac{FE^{'}}{1 - e^{-\frac{FE^{'}T}{V_{ees}}} Z^{-1}} + \alpha \quad C_a(Z) + E(Z) \qquad (6)$$

or

$$C_{tis}(Z) - e^{-\frac{FE^{'}T}{V_{ees}}} \cdot Z^{-1} C_{tis}(Z) =$$

$$(FE^{'} + \alpha) C_a(Z) - \alpha e^{-\frac{FE^{'}T}{V_{ees}}} \cdot Z^{-1} C_a(Z) + (1 - e^{-\frac{FE^{'}T}{V_{ees}}} \cdot Z^{-1}) E(Z) \qquad (7)$$

which can be written as:

$$C_{tis}(Z) - b_1 Z^{-1} C_{tis}(Z) = a_0 C_a(Z) - a_1 Z^{-1} C_a(Z) + \eta(Z) \qquad (8)$$

in which:

$$b_1 = e^{-\frac{FE^{'}T}{V_{ees}}}, \quad a_0 = FE^{'} + \alpha, \quad and \quad a_1 = -\alpha e^{-\frac{FE^{'}T}{V_{ees}}} \qquad (9)$$

or

$$\alpha = -\frac{a_1}{b_1}, \quad FE^{'} = a_0 + \frac{a_1}{b_1}, \quad and \quad V_{ees} = \frac{a_0 + \frac{a_1}{b_1}}{-\ln b_1} \qquad (10)$$

and $\eta(Z)$ is colored noise. From equation (8) we can calculate the transfer function of the system:

$$H(Z) = \frac{C_{tis}(Z)}{C_a(Z)} = \frac{a_0 + a_1 Z^{-1}}{1 - b_1 Z^{-1}} \qquad (11)$$

which is an ARMA(1,1), i.e., autoregressive moving average with one zero and one pole. Now let us transform equation (8) back to the time domain to get:

$$C_{tis}(n) - b_1 C_{tis}(n-1) = a_0 C_a(n) + a_1 C_a(n-1) + \eta(n) \qquad (12)$$

which is an ARMA in the time domain and can be solved by any of the existing methods, e.g., least mean square (LMS), maximum a posteriori (MAP), Maximum Likelihood and Levinson. Here we show how the LMS works. We may write the output noise power as:

$$E = \sum_{n=0}^{N-1} \eta^2(n) \qquad (13)$$

in which N is the number of samples. Substituting $\eta(n)$ from equation (12), we get:

$$E = \sum_{n=0}^{N-1} \{C_{tis}(n) - b_1 C_{tis}(n-1) - a_0 C_a(n) - a_1 C_a(n-1)\}^2 \qquad (14)$$

In order to minimize *E*, we should have:

$$\frac{\partial E}{\partial b_1} = 0, \quad \frac{\partial E}{\partial a_0} = 0, \quad and \quad \frac{\partial E}{\partial a_1} = 0 \qquad (15)$$

or

$$\begin{cases} b_1 \sum_{n=1}^{N-1} C_{tis}{}^2(n-1) + a_0 \sum_{n=1}^{N-1} C_a(n) \cdot C_{tis}(n-1) + a_1 \sum_{n=1}^{N-1} C_a(n-1) \cdot C_{tis}(n-1) = \sum_{n=1}^{N-1} C_{tis}(n) \cdot C_{tis}(n-1) \\ b_1 \sum_{n=1}^{N-1} C_{tis}(n-1) \cdot C_a(n) + a_0 \sum_{n=1}^{N-1} C_a{}^2(n) + a_1 \sum_{n=1}^{N-1} C_a(n-1) \cdot C_a(n) = \sum_{n=1}^{N-1} C_{tis}(n) \cdot C_a(n) \\ b_1 \sum_{n=1}^{N-1} C_{tis}(n-1) \cdot C_a(n-1) + a_0 \sum_{n=1}^{N-1} C_a(n) \cdot C_a(n-1) + a_1 \sum_{n=1}^{N-1} C_a{}^2(n-1) = \sum_{n=1}^{N-1} C_{tis}(n) \cdot C_a(n-1) \end{cases} \qquad (16)$$

Solving Equations (16) (3 equations with 3 unknowns), we find the LMS estimation of a_0, a_1, and b_1, then we can calculate the estimation of α, $FE^{'}$, and V_{ees}, using equations (10).

2.2 Experimental Procedures

2.2.1 Simulations

To test the theory and evaluate the robustness of the method to measurement noise, we conducted a simulation study. In this study, we started with a reasonable $C_a(t)$ and nominal values for $FE^{'}$, α, r, and V_{ees}. By numerically convolving the kernel with $C_a(t)$ and adding random white Gaussian noise with varying powers, we generated different sets of data with different signal-to-noise ratio (SNR). We then used the resulting data to solve (16) and estimate α, V_{ees}, and $FE^{'}$.

2.2.2 An Animal Model of Cerebral Tumor

A human glioma cell line was implanted in an athymic nude rat. Cells were maintained by serial passage in vitro using Dulbecco's medium and 10% fetal calf serum. The rat's head was immobilized using a small animal stereotactic device. Following a midline incision, the skull was exposed. A burr hole was drilled through the skull taking care not to penetrate the dura. Five hundred thousand U251MGn human glioma cells in 5μl were injected at a rate of 1μl/min into a location 2.5mm anterior to the bregma, 2.0mm to the right of the midline and a depth of 3.0 mm. About three weeks after implantation, the animal was imaged in a 7 Tesla magnet.

2.2.3 MRI Procedures

We have developed an imaging protocol on 7 Tesla animal system employing the TOMROP [10] sequence, which is an imaging version of the Look-Locker technique [11] for determining T1. At least one dummy cycle was applied before the start of data acquisition. Inversion of the longitudinal magnetization was accomplished using a non-selective hyperbolic secant adiabatic pulse of duration 12 ms. One phase-encode line of 16 small-tip-angle gradient-echo images (TE 4 ms) was acquired after each such adiabatic inversion, at 40 ms intervals, for a total recovery time of 640 ms with 500 ms relaxation interval between each adiabatic inversion. Matrix size was 128X64, FOV 32 mm, and three 2 mm slices were imaged. Total imaging time per data set was 84 sec, allowing the formation of maps of R1 at intervals of less than 90 sec.

Look-Locker procedures result in a set of images which recover with a time constant T1* toward a steady-state magnetization. T1* and the steady-state magnetization both have a dependency on the tip-angle of the readout, as well as on T1 and the equilibrium magnetization. Thus, estimating the parameters of interest requires an optimization procedure to estimate for each slice the parameters of interest and a 'nuisance' variable, the tip-angle. Home-written software employing a Simplex curve-fitting algorithm, as explained in Gelman, [12], but with a non-negative constraint added, was used for all such procedures. This generated R1 maps for each slice every 90 seconds.

3. RESULTS

3.1 Simulation Study

Accuracy of estimates were evaluated and graphed in Fig. 1, illustrating robustness of the proposed method. The estimation is unbiased and the standard deviation of each estimation is shown as SNR changes.

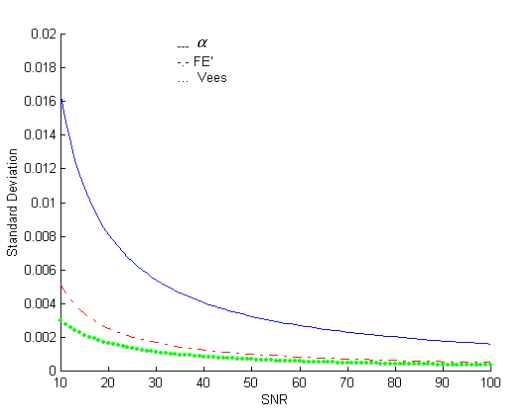

Figure 1. Standard deviation of estimated parameters in different SNR levels. Nominal values: α=0.02, $FE^{'}$=0.2, V_{ees}=0.085

3.2 Animal Study

The pixel intensity of the R1 maps generated in the previous section are proportional to the concentration of the contrast agent in each voxel. Therefore equation (1) holds for the sequence of R1 maps. Using a region of interest on the sagittal sinus, we obtained R1 values proportional to $C_a(t)$. Solving the linear system of equations (16) with the results, we generated maps of α, $FE^{'}$ and V_{ees} as shown in Fig. 2-4. These maps show a good compromise with the T1-weighted image shown in Fig. 5 so they are useful for other applications.

4. SUMMARY AND CONCLUSIONS

We have developed a new deconvolution method for estimating permeability from MRI. The proposed approach translated the problem into the ARMA parameter estimation through the application of the Z-transform to the discrete version of the underlying perfusion model. We illustrated accuracy and robustness of the proposed method through its application to a simulation study. We also showed practical utility of the method by applying it to the MRI of an animal model of brain tumor. The proposed method processes the R1 maps for permeability estimation. Further development of the method to process T1-weighted images, thereby avoiding R1 maps estimation, is a direction for the future work. Comparison of the permeability estimated from MRI to that of autoradiography is another direction for the future work.

5. REFERENCES

[1] P.S. Tofts: "Modeling Tracer Kinetics in Dynamic Gd-DTPA MR Imaging," *Journal of Magnetic Resonance Imaging*, vol. 7, pp. 91-101, 1997.

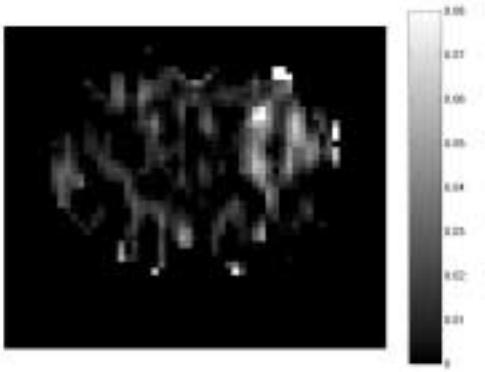

Figure 2. Map of α estimated by ARMA model from R1 maps.

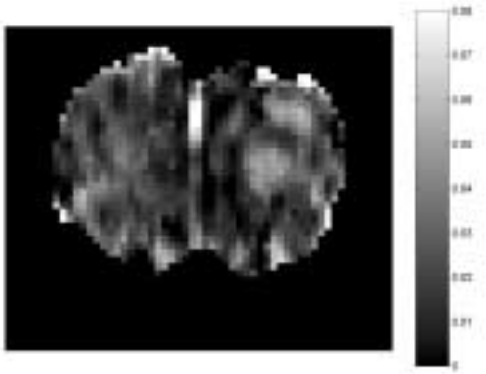

Figure 3. Map of FE' estimated by ARMA model from R1 maps.

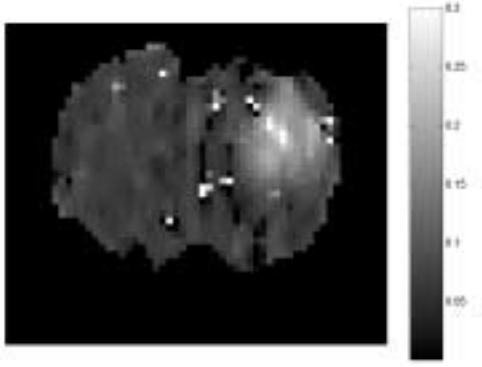

Figure 4. Map of V_{ees} estimated by ARMA model from R1 maps.

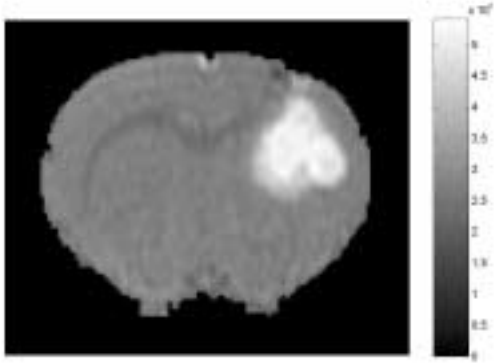

Figure 5. T1-weighted image of rat brain used for estimation of permeability parameters.

[2] P. Tofts and A. Kermode: "Measurement of the blood-brain barrier permeability and leakage space using dynamic MR Imaging. Fundamental Concept," *Magnetic Resonance in Medicine*, vol. 17, pp. 357-367, 1991.

[3] E. Henderson et al., "Simultaneous MRI Measurement of Blood Flow, Blood Volume, and Capillary Permeability in Mammary Tumors using Two Different Contrast Agents," *Journal of Magnetic Resonance Imaging*, vol. 12(6), pp. 991-1003, 2000.

[4] H. Larsson et al., "Quantitation of blood brain barrier defect by Magnetic resonance Imaging and Gadolinium-DTPA in Patients with Multiple Sclerosis and Brain Tumors," *Magnetic Resonance in Medicine*, vol. 16, pp. 117-131, 1990.

[5] G. Brix et al., "Pharmacokinetic parameters in CNS Gd-DTPA enhanced MR imaging," *Journal of computer assisted tomography*, vol. 15, pp. 621-628, 1991.

[6] P.S. Tofts, et al., "Estimating kinetic parameters from dynamic contrast-enhanced T(1)-weighted MRI of a diffusable tracer: standardized quantities and symbols," *J Magn Reson Imaging*, vol. 10(3), pp. 223-32, 1999.

[7] C. Crone, "The Permeability of Capillaries in Various Organs as Determined by Use of the Indicator Diffusion Method," *Acta physiol scand*, vol. 58, pp. 292-305, 1963.

[8] N. Lassen and W. Perl, *Tracer Kinetic Methods in Medical Physiology*, 1 ed. 1979, New York, N.Y.: Raven Press.

[9] N. Lassen, and W. Perl, "Multiple Indicators: Capillary Permeability in Tracer Kinetic Methods," *Medical Physiology*, pp. 156-175, 1979.

[10] G. Brix et al., "Fast and Precise T1 Imaging Using a TOMROP Sequence," *Magnetic Resonance Imaging*, vol. 8, pp. 351-356, 1990.

[11] D.C. Look and D.R. Locker, "Time Saving in Measurement of NMR and EPR Relaxation Times," *Review of Scientific Instruments*, vol. 41(2), pp. 250-251, 1970.

[12] N. Gelman et al., "Interregional Variation of Longitudinal Relaxation Rates in Human Brain at 3.0 T: Relation to Estimated Iron and Water Contents," *Magnetic Resonance in Medicine*, vol. 45,pp. 71-79, 2000.